GEOPHYSICAL RESEARCH LETTERS, VOL. 28, NO. 16, PAGES 3211-3214, AUGUST 15, 2001

Regional-Scale Permeability by Heat Flow Calibration in the Powder River basin, Wyoming

Brian J. O. L. McPherson,[1] Peter C. Lichtner,[2] Craig B. Forster,[3]
Barret S. Cole[1]

Abstract. Forward modeling of coupled fluid and heat flow in the Powder River basin, Wyoming, is used to explain anomalously high heat flow values observed in the southern portion of the basin. Effective basin-scale permeabilities of selected Powder River basin aquifers and aquitards were calibrated by matching surface heat flow measurements to simulation results. Fractures associated with a large anticline in the southwestern part of the basin were found to play a major role in the basin's thermal regime. While the model results are non-unique, they demonstrate that regional structural features play an important role in a basin's overall energy budget and fluid flow regime. With the results of the basin-scale model it is possible to evaluate regional-scale flow and transport processes.

1. Introduction

Coupled heat flow and subsurface fluid flow in advective thermal regimes makes it possible to use thermal observations to constrain hydrodynamics. For example, many investigators have correlated variations in heat flow and temperature data to hydrodynamic patterns (Majorowicz and Jessop, 1981; Chapman et al., 1984; Willett and Chapman, 1987; Clauser and Villinger, 1990; Gosnold, 1990; Person and Garven, 1992). Other investigators estimate ranges of fluid flow rates or permeability based on variations in the thermal regime (Bredehoeft and Papadopulos, 1965; Willett and Chapman, 1987; Ingebritsen et al., 1989; Deming, 1993).

In this study, forward modeling of coupled fluid and heat flow in the Powder River basin is used to explain significant anomalies in an otherwise conductive thermal regime. Basin-scale aquifer permeability is calibrated to surface heat flow observations. Two different models are considered based on homogeneous and heterogeneous representations of basin permeability.

2. Geologic Setting

The Powder River basin is located in northeastern Wyoming and southeastern Montana, and is $\sim$ 30,000 km^2 in size. The basin is bounded by the Bighorn Mountains to the west and the Laramie Mountains to the south. The Black Hills partially bound the basin to the east, and the Yellowstone River marks the northern boundary of the basin in Montana. Surface water drains from southwest to northeast, because the southwestern half of the basin has slightly higher elevation. A generalized southwest-northeast cross-section (A-A') through the Powder River basin is shown in Figure 1a. The asymmetric structure of profile A-A' prevails through most of the basin. The general stratigraphy of the basin includes alternating sandstones, shales, and carbonates, as described by McPherson and Chapman (1996). To simplify analyses, McPherson and Chapman (1996) grouped specific formations into eight units, as delineated in Figure 1a, and we used these same eight units in this study.

2.1. Thermal Regime

McPherson and Chapman (1996) estimated both the 3-dimensional temperature field and the surface heat flow distribution within the southern Powder River Basin. The average surface heat flow in the region is 52 mW m^{-2}, and generally varies between 40 and 60 mW m^{-2}. However, anomalously high heat flow values (greater than 200 mW m^{-2}) observed in the vicinity of the Salt Creek Anticline cannot be explained by conductivity variation alone.

The distribution of surface heat flow for profile A-A' is plotted in Figure 1b. The general heat flow trend mimics the basin's regional-scale structure, including a slight dip in the thermal signature at the synclinal axis of the basin. Exceptions to this trend include very high heat flow values in the vicinity of the Salt Creek Anticline (225 mW m^{-2}), about 25 km NE of A (Figure 1), and an abrupt decrease in heat flow occurring at the northeastern part of the transect (between profile distances 150 km and 180 km).

McPherson and Chapman (1996) inferred that the first order thermal pattern observed (Figure 1b) is caused by preferential conductive refraction of heat through basement strata, which have higher thermal conductivity than the sedimentary section. Both depositional and erosional effects were determined to be small (<5 mW m^{-2}) and only partially contribute to the non-conductive thermal signature.

We hypothesize that meteoric water recharged in the Black Hills causes the depressed surface heat flow in the northeastern part of profile A-A' (Figure 1). Groundwater from this area is topographically driven deep in the basin where it is warmed by ambient heat. The heated groundwater is subsequently driven up-dip on the southwest side of the basin axis and discharged in the area of the Salt Creek Anticline, elevating the surface heat flow in that area to > 200 mW m^{-2}. We used a mathematical model of coupled fluid flow and heat transfer to test this hypothesis.

3. Numerical Model

We assembled a numerical model of the Powder River basin and simulated a range of different regional permeabil-

[1]New Mexico Institute of Mining and Technology, Department of Earth and Environmental Science, Socorro, NM.
[2]Los Alamos National Laboratory, Earth & Environmental Sciences Division, (EES-6) MS F-649, Los Alamos, NM.
[3]University of Utah, Department of Geology and Geophysics, Salt Lake City, UT.

Paper number 2000GL012591.
0094-8276/01/2000GL012591$05.00

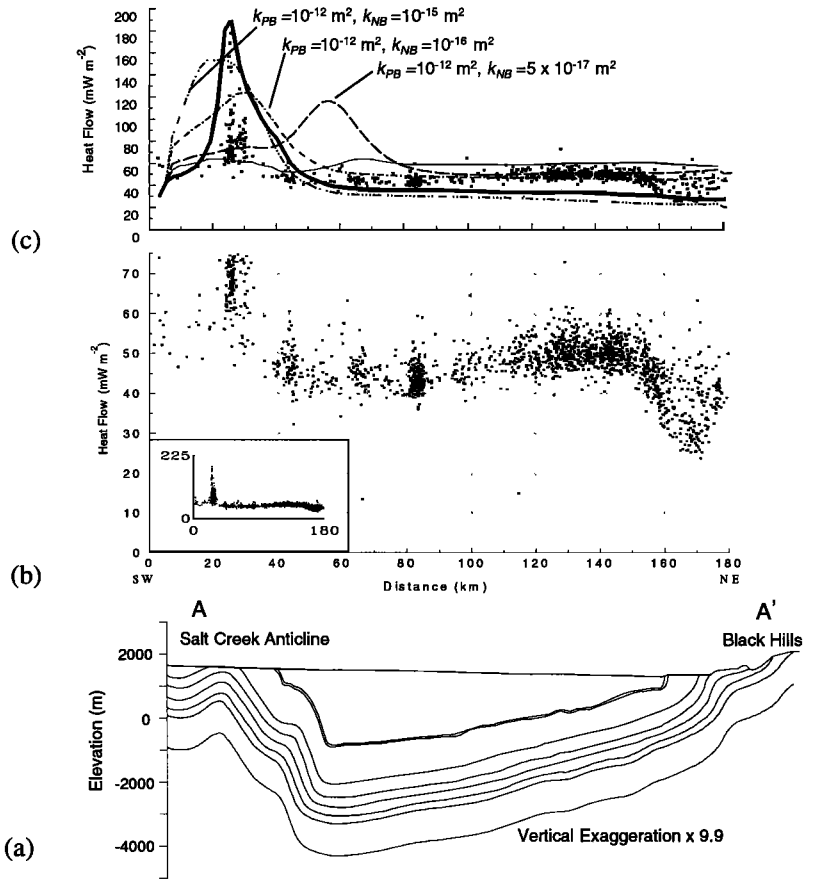

Figure 1. (a) Powder River Basin structural cross-section A-A'; (b) observed heat flow in basin; (c) results of the coupled groundwater-heat flow model simulations. The text provides details of each indvidual plot.

ity distributions to determine whether regional groundwater flow could be responsible for apparently non-conductive aspects of the observed thermal regime. The basin's structure in relation to surrounding topography suggests that regional groundwater flow in the Powder River basin is two-dimensional, N-NE to S-SW, and this possibility is corroborated by the study of Hagmaier (1971) as well as surface drainage patterns. Additionally, while cross-flow in a three-dimensional flow system cannot be completely ruled out, sufficient data to assemble an adequate three-dimensional model were not available. Thus, we evaluated the system using a two-dimensional finite difference model of cross-section A-A' (Figure 1), coincident with the locus of surface drainage of the basin. The model domain is 230 km horizontal by 5 km vertical, consisting of 5000 grid-blocks (100 horizontal by 50 vertical), each 2300 m by 100 m. Eight model units are delineated in the cross-section of Figure 1a. These eight units comprise the different regions of homogeneous permeability and thermal conductivity included in the model.

We used the numerical simulator TOUGH2, an integrated finite difference model that simulates coupled heat and fluid transport in variably saturated porous or fractured media (Pruess, 1991). Fluid flow is described with a multiphase extension of Darcy's law, and heat flow occurs by conduction and advection. For a complete description of the numerical model, its algorithm, governing equations and solution method, see Pruess (1991).

3.1. Model Parameterization

All thermal data used to parameterize the model are drawn from McPherson and Chapman (1996), who provide details of those data. Core- and well-scale permeability and porosity of selected Powder River Basin sandstone units are tabulated by Lawyer et al. (1981), but reliability of these data is unknown. Permeability and porosity data for Powder River Basin shale units are scarce or non-existent. However, at least two studies, Neuzil (1994) and Bredehoeft et al. (1983), have analyzed the permeability of the Pierre Shale (Upper Cretaceous) in central South Dakota. We used the data of Lawyer et al. (1981), Neuzil (1994) and Bredehoeft et al. (1983) only to guide design of our model sensitivity analysis. We assigned an exponential decrease in porosity with depth, as outlined by Sclater and Christie (1980).

3.2. Boundary Conditions and Initial Conditions

Maps and cross-sections by Rankl and Lowry (1990) and Hagmaier (1971) indicate that the water table lies within 100 m of the surface. Thus, we assumed the top surface of the model domain to be a Dirichlet-type boundary (constant head), with head assigned equal to the value of topographic elevation minus 100 meters. Basement rocks below the Madison Group (bottom unit illustrated in Figure 1a), are a no-flow (Neumann) boundary for fluid, but are a constant flow (Neumann) boundary for heat. The background

regional heat flow uniformly assigned to the bottom boundary is 52 mW m^{-2}, the average heat flow for the region determined by McPherson and Chapman (1996). The northeastern side boundary (right side of cross-section A-A'; Figure 1a) is assumed no fluid flow (Neumann), as it is a symmetry point in topography in the Black Hills. The southwestern side boundary (left side of Figure 1a) is assigned constant groundwater head (Dirichlet), with head set equal to the surface elevation at that point. Land surface temperatures (top boundary) were held constant, set at values listed in a compendium of surface temperature data published by the National Oceanic and Atmospheric Administration (NOAA, 1989). The side model domain boundaries are assumed insulated with respect to temperature. Initial conditions for the model include hydrostatic head and conductive temperature distributions.

4. Model Results and Discussion

In a sensitivity study, specific ranges of permeability were evaluated in a series of model runs while holding all other variables constant. We assigned selected values of homogeneous, anisotropic permeability to all units, e.g., a homogeneous and anisotropic whole basin model, and compared resulting modeled surface heat flow distributions to the observed distribution (Figure 1b). An upper limit of permeability parallel to bedding, k_{PB}, equal to 10^{-12} m^2 was chosen because the measured permeabilities (Lawyer et al., 1981) do not exceed 10^{-12} m^2. Additionally, we varied anisotropy ratios of permeability parallel to bedding versus permeability normal to bedding, or k_{PB}:k_{NB}, from 0 to 3 orders of magnitude difference (Bethke, 1985).

Figure 1c illustrates the heat flow results produced by some of these models. The non-bold solid line corresponds to a model with $k_{PB} = 10^{-14}$ m^2 and $k_{NB} = 5 \times 10^{-17}$ m^2, and this permeability is low enough that conduction appears to dominate the thermal regime. The remaining lines, excepting the bold solid line, correspond to models with stepwise increasing anisotropy: $k_{PB} = 10^{-12}$ m^2 : $k_{NB} = 10^{-15}$ m^2 (dot-dot-dot-dash), $k_{PB} = 10^{-12} m^2$: $k_{NB} = 10^{-16}$ m^2 (dot-dash), $k_{PB} = 10^{-12} m^2$: $k_{NB} = 5 \times 10^{-17}$ m^2 (long dash). In these models, a simple basin-scale flow system results in which fluid flows from the Black Hills to deep in the basin, and then travels up the southwest side of the basin axis, discharging in the area of the Salt Creek Anticline. Advection carries heat from deep in the basin up the anticline. As anistropic ratio increases, the character of the flow system changes, including a shift in the upward-flow portion of the flow system northeastward toward the basin axis. With this shift comes a less dramatic advective signature. The conserved heat budget reduces the "spike" in heat flow, and it becomes broader, less focused, and background heat flow is increased elsewhere. This suggests that the best choice of k_{PB} for a homogeneous model, among those used in the sensitivity analysis, is approximately 5×10^{-12} m^2, with the anisotropy about 3 orders of magnitude, or $k_{NB} \sim 10^{-15}$ m^2 to 5×10^{-16} m^2.

4.1. Heterogeneous Model

None of the homogeneous models provided a strong match to the observed surface heat flow distribution. To improve the fit to the heat-flow data a heterogeneous model was considered. Specifically, we identified major shale units and major sandstone and carbonate units, and assigned the best k_{NB}:k_{PB} value (i.e., that which produced heat flow results most consistent with the observations) from the homogeneous model sensitivity analysis to the sandstone and carbonate units. We assigned the shale units to be tight "confining layers" with an isotropic permeability ($k_{NB} = k_{PB}$) of 10^{-20} m^2, which is the lab-scale permeability measured for the Pierre Shale (in North Dakota) by Neuzil (1994).

This initial heterogeneous model did no better in matching surface heat flow than the homogeneous models (Figure 1c). However, Love and Christiansen (1985) indicate the presence of surface joints in the vicinity of the Salt Creek Anticline. To account for this possibility we arbitrarily assigned an isotropic permeability, $k_{NB} = k_{PB} = 10^{-12}$ m^2, to strata within the anticline to simulate a locally high fracture permeability. This simple heterogeneous model provided a surface heat flow distribution (Figure 1c, bold solid line) that matched the observed heat flow pattern much better than the first heterogeneous model and any of the homogeneous models. Flow vectors indicate relatively high groundwater flow rates, approaching 10^{-2} m/year, through basal aquifers of the model, including the Minnelusa/Tensleep sandstones, the Pahasapa Limestone, the Madison Limestone and the Deadwood Formation. On the southwest limb of the basin syncline, the magnitudes of flow vectors are higher because the conduit thins relative to the northeast side. Flow magnitudes in the basin model range from $\sim 10^{-4}$ m/year up to $\sim$1 m/year, and are higher in the apex of the Salt Creek Anticline due its high permeability. The model providing "best fit" to the heat flow data (Figure 1c) defines well the upper bound of the heat flow data, but the simulation does not provide a good explanation for the remaining considerable scatter in observed heat flow at the crest of the anticline. It is likely that not all of the heat flow observations sample the highly permeable zones. This scatter may represent more conductively-dominated thermal conditions and/or effects of local recharge by precipitation at the surface. We did not quantitatively investigate effects of infiltration or precipitation.

Finally, our modeling results suggest that the regional-scale permeability of the Pierre Shale and other shale units in the Powder River Basin is several orders of magnitude lower than that of the Pierre Shale in South Dakota determined by Bredehoeft et al. (1983).

5. Conclusions

Using forward modeling of coupled fluid and heat flow in the Powder River Basin, it was possible to estimate basin-scale aquifer permeability by calibrating the model against heat-flow anomalies in an otherwise conductive thermal regime of the basin. Model results demonstrated that basin shape and regional scale geologic features play a significant role in causing heat flow anomalies. Such modeling can be used to investigate regional scale flow and transport patterns, for example, those associated with geologic sequestration of carbon dioxide. Specifically, we concluded that:

1) Advection by a regional scale groundwater flow system can explain anomalies in an otherwise conductive surface heat flow distribution. In other words, conductive portions and advective portions of the regional surface heat flow distribution may be distinguished from each other.

2) Results of this study demonstrate that anomalous heat flow may be used to determine the presence of zones of high permeability associated with regional-scale geologic structures. For example, extremely high heat flow values (>200 mW m^{-2}) observed over the Salt Creek Anticline in the Powder River Basin were matched only when simulating the structure as a high permeability region due to associated fractures.

3) Although the model results are non-unique, they demonstrate that basin shape and regional structural features play a significant role in a basin's fluid flow regime, surface heat flow patterns, and its overall energy budget.

References

Bethke, C. M., A numerical model of compaction-driven groundwater flow and heat transfer and its application to the paleohydrology of intracratonic sedimentary basins, J. Geophys. Res., 90, 6817-6828, 1985.

Bredehoeft, J. D., C. E. Neuzil, and P. C. D. Milly, Regional flow in the Dakota aquifer: a study of the role of confining layers, U.S. Geol. Surv. Water Supply Pap. 2237, 1983.

Bredehoeft J. D. and I. S. Papadopulos, Rates of vertical groundwater movement estimated from the Earth's thermal profile, Water Resources Research, 1, 325-328, 1965.

Chapman, D. S., T. H. Keho, M. S. Bauer, and M. D. Picard, 1984, Heat flow in the Uinta Basin determined from bottom hole temperature (BHT) data, Geophysics, v. 49, p. 453-466.

Clauser, C., and H. Villinger, Analysis of conductive and convective heat transfer in a sedimentary basin, demonstrated for the Rheingraben, GEOPHYS. J. INT., 100, 393-414, 1990.

Deming, D., Regional permeability estimates from investigations of coupled heat and groundwater flow, North Slope of Alaska, J. Geophys. Res., 98, 16271-16286, 1993.

Gosnold, W. D., Jr., Heat flow in the Great Plains of the United States, J. Geophys. Res., 95, 353-374, 1990.

Hagmaier, J. L., Groundwater flow, hydrochemistry, and uranium deposition in the Powder River Basin, Wyoming, Ph. D. Thesis, University of North Dakota, 1971.

Ingebritsen, S. E., D. R. Sherrod, and R. H. Mariner, Heat flow and hydrothermal circulation in the Cascade Range, north-central Oregon, Science, 243, 1458-1462, 1989.

Lawyer, G. F., J. Newcomer, and C. Eger, Powder River Basin Oil and Gas Fields, pp. 1-472, Wyo. Geol. Assoc., Casper, WY, 1981.

Love, J. D., and A. C. Christiansen, Geologic Map of Wyoming, U. S. Geol. Survey, Reston, Va., 1985.

Majorowicz, J. A., and A. M. Jessop, Regional heat flow patterns in the western Canadian sedimentary basin, Tectonophysics, 74, 209-238, 1981.

McPherson, B.J.O.L. and Chapman, D.S., 1996, Thermal Analysis of the Southern Powder River Basin, Wyoming, Geophysics, 61:1689-1701.

National Oceanic and Atmospheric Administration, Wyoming Climatological Data, Volume 98, Number 1, 1989.

Neuzil, C. E., How permeable are clays and shales?, Water Resources Research, 30, 145-150, 1994.

Person, M., and G. Garven, Hydrologic constraints on petroleum generation within continental rift basins: Theory and applications to the Rhine Graben, AAPG Bull., 76, 468-488, 1992.

Pruess, K., TOUGH2–a general-purpose numerical simulator for multiphase fluid and heat flow, Rep. LBL-29400, Lawrence Berkeley Lab., September 1991.

Rankl, J. G., and M. E. Lowry, Ground-water-flow systems in the Powder River structural basin, Wyoming and Montana, U. S. Geological Survey Water-Resources Investigations Report 85-4229, 1990.

Sclater, J. C., and P. A. F. Christie, Continental stretching: an explanation of the post-mid-Cretaceous subsidence of the central North Sea basin, J. Geophys. Res., 85, 3711-3739, 1980.

Willett, S. D., and D. S. Chapman, On the use of thermal data to resolve and delineate hydrologic flow systems in sedimentary basins: an example from the Uinta Basin, Utah, in Proceedings of the Third annual Canandian/American Conference on Hydrogeology; Hydrology of Sedimentary Basins—Applications to Exploration and Exploitation, edited by B. Hitchon, S. Bachu, and C. Sauveplane, pp. 159-168, National Water Well Assn., Dublin, Ohio, 1987.

Barret S. Cole, Brian J. O. L. McPherson, New Mexico Institute of Mining and Technology, Hydrology Program, Department of Earth and Environmental Science, Socorro, New Mexico 87801 (e-mail: brian@nmt.edu)

Craig B. Forster, University of Utah, Department of Geology and
Geophysics, Salt Lake City, UT 84112 (e-mail: cforster@mines.utah.edu)

Peter C. Lichtner, Los Alamos National Laboratory, Earth and Environmental Sciences Division, (EES-6) MS F-649, Los Alamos, NM 87545 (e-mail: lichtner@lanl.gov)

(Received November 06, 2000; revised April 12, 2001; accepted May 22, 2001.)